Ultrasonics 99 (2019) 105953

Contents lists available at ScienceDirect

Ultrasonics

journal homepage: www.elsevier.com/locate/ultras

Modeling guided wave propagation in functionally graded plates by state-vector formalism and the Legendre polynomial method

Jie Gao[a], Yan Lyu[a,*], Mingfang Zheng[b], Mingkun Liu[a], Hongye Liu[c], Bin Wu[a], Cunfu He[a]

[a] College of Mechanical Engineering and Applied Electronics Technology, Beijing University of Technology, Beijing, China
[b] School of Environment and Civil Engineering, Dongguan University of Technology, Dongguan 523808, China
[c] School of Optical-Electrical and Computer Engineering, University of Shanghai for Science and Technology, Jungong Road 580, Shanghai 200093, China

ARTICLE INFO

Keywords:
Legendre polynomial method
Guided waves
Dispersion curves
Functionally gradient material

ABSTRACT

A numerical method is presented for the investigation of the propagation characteristic of guided waves in functionally gradient material (FGM) plates. Based on the State-vector formalism and Legendre polynomial method, the typical non-stratified computing of dispersion curves of FGMs is realized, by introducing the univariate nonlinear regression to optimize the arbitrary gradient distribution of material component. Comparing with the conventional Matrix method, the proposed method avoids the exhausting root-locating algorithm of solving the transcendental equation by a single-variable scanning process. This method turns it into an algebraic eigenvalue problem, which mainly depends on the orthogonal completeness and strong recursive property of Legendre polynomial series. It provides a fast and flexible approach to extracting the dispersion curves, displacement distribution and stress profile, simultaneously. Results from chrome-ceramic FGM plate are compared with those from the previous articles to confirm the feasibility and accuracy of the proposed method. Then, this approach is further applied to iron based alumina FGM. The dispersion curves with different gradient function are calculated to illustrate the influence of the gradient variation. Moreover, the influence of the cut-off order of Legendre orthogonal polynomials on the convergence of dispersion curves is also revealed through numerical examples. Utilizing the mapping relationship between the gradient distribution and the propagation characteristics, it gives theoretical support for nondestructive evaluation and quantitative estimation of the structural characteristics of FGM plates.

1. Introduction

With the development of nowadays material science, material structures are becoming more and more complex and delicate. Functionally gradient material (FGM), as a key fundamental material, has recently received considerable attention in aerospace, mechanical engineering, etc., due to its strong designability [1]. It's of great importance to develop a nondestructive testing method to realize the characterization of mechanical properties of FGMs. As well known, ultrasonic wave propagation carries much information about the material, which gives a chance to characterize the material performance [2]. Aiming at the non-destructive evaluation, investigating the wave propagation behavior in FGM plate has become a topic of practical research.

In recent years, several analytical and computational studies have been extended on the properties of functionally graded materials. Based on the modified couple-stress theory, Guo analyzed numerically the size-dependent behavior of the functionally graded material under load, such as functionally graded anisotropic elastic composites [3], and layered model for simply-supported and functionally graded magneto-electro-elastic plates [4]. Sladek developed meshless local Petrov-Galerkin (MLPG) method to investigate magneto-electric coefficient of FGM composite with a pure piezo-magnetic and piezoelectric behavior on the lower and upper surface, respectively [5]. Then, Sladek applied MLPG method to bending analysis of FGM plates with integrated magneto-electro-elastic sensor and actuator layer [6]. Moreover, Wang researched the response of functionally graded material multiferroic composites under different type of loads by using three-dimensional finite element method [7]. At recent, starting with the microscopic composition, Bishay [8] discussed the effect of the material property ratio and lattice mismatch strain ratio on electromechanical behavior of Functionally Graded Quantum Dots with and without wetting later. In addition, with the purpose of non-destructive evaluation, the wave characteristics in FGM structures have also attracted considerable

* Corresponding author.
E-mail address: lvyan@bjut.edu.cn (Y. Lyu).

https://doi.org/10.1016/j.ultras.2019.105953
Received 18 February 2019; Received in revised form 15 June 2019; Accepted 25 June 2019
Available online 04 July 2019
0041-624X/

researchers.

Likewise, numerous approaches have been also used to analyze the acoustic wave propagation in FGM plates, which usually divided the gradient structure into sublayers with homogeneous properties along the thickness direction. Liu [9] developed a finite layer element method to analyze the propagation characteristics of Lamb waves in FGM plate. Then, Ohyoshi [10] improved the finite layer element into the linearly interpolation layer element (LIE) to approximate the continuous gradient variation. Moreover, Liu [11] derived the general solution of LIE model, and investigated the propagation characteristics of stress waves in FGM plate by using the continuity conditions. On this basis, Han [12] proposed a quadratic layer element method to analyze the stress waves in FGM plates, and obtained the material properties of an actual SiC-C FGM plate by means of the genetic algorithm. Chen [13] adopted an accurate laminate to reconstruct the target FGM plate, then the reverberation matrix method was employed to investigate the dispersion characteristics [14]. Afterwards, Salah [15] used the stiffness matrix method to analyze the propagation of Love waves over a half space of an elastic substrate covered by a functionally gradient piezoelectric material (FGPM) plate. In all the above mentioned researches, the FGMs were divided into many homogeneous or inhomogeneous layers in order to solve the wave propagation problem. Obviously, the layer number of FGM plays a vital role in the numerical accuracy of calculations.

The introduction of the asymptotic analysis method provides a new idea for the study of wave dispersion behavior of FGM plates, such as the WKB (Wentzel–Kramers–Brillouin) method, orthogonal polynomial expansion method, power series technique, and so on. Li [16] computed the dispersion relations of Love waves in a semi-finite elastic solid covered with FGPM medium with the electric open and short cases through the WKB method. Likewise, Qian [17] also used the WKB method to investigate the dispersion behavior of the Love wave propagation in a piezoelectric half space covering a FGM layer. Lefebvre and Elmainouni developed Legendre polynomial series method to calculate the dispersion curves and displacement distribution of guided waves in FGM plate [18] and radially gradient cylinders [19]. Later on, Yu extended this method to illustrate the guided wave problem of more complex structures, such as thermoelastic [20], viscoelastic FGM plates [21] and functionally gradient piezoelectric-piezomagnetic plates [22]. In addition, Cao analyzed the mapping relations between the gradient characteristics with the dispersion curves of guided waves in FGM [23] and FGPM plates [24] by using the power series technique. Similarly, the high-order Chebyshev polynomials as approximation functions were also used to solve the wave problem of FGM plate. Hedayatrasa [25] numerically modeled the propagation behavior of elastic waves in 2D FGMs using the time-domain spectral finite element method based on the Chebyshev Lagrangian expansion. As mentioned above, the studies were treating the FGM structures as a continuously gradient medium, and effectively calculated the propagation characteristics of acoustic waves in FGM plates without separating it into multilayer plates. In addition, Spectral Collocation Method [26], Semi-Analytical Finite Element method [27,28] have been also developed to model guided waves propagation in waveguides with complex cross sections significantly, which includes complicated geometries and complex material properties. Nevertheless, few literatures paid attention to the non-destructive testing and evaluation of the characteristics of FGM plates. And above all, the development of accurate and efficient calculation of dispersion curves with the associated displacement and stress profiles should be most important. So, more reliable and robust approaches are still needed to enhance the accuracy and efficiency in establishing the theoretical model and analyzing the complicated propagation of guided waves for FGMs.

Previously, we have studied the wave propagation in anisotropic plates [29] and anisotropic hollow cylinders [30] by Legendre polynomial solution based on state-vector formalism. Now, we attempt to investigate the wave propagation in FGM plates with different gradient types. The gradient shape of the mechanical properties are fitted optimally through univariate nonlinear regression. The dispersion curves are calculated and compared with the published data. Then, the case of iron based alumina FGM is given to validate the flexibility of the proposed method. The effects of different gradient function on the dispersion curves and stress distribution are also illustrated. In addition, the influence of the cut-off order of Legendre orthogonal polynomials on the convergence of the numerical results is discussed in details.

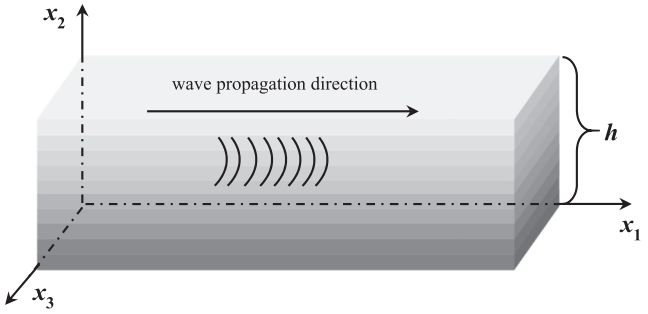

Fig. 1. Geometry of the FGM plate.

2. Problem statement

Consider an FGM plate with varying material properties (density ρ and elastic constants C_{IJ}, in which I and J ranges from 1 to 6) with regard to thickness h ($0 \le x_2 \le h$), which is infinite horizontally but finite in the x_2 direction, as shown in Fig. 1, and the guided waves propagate along the x_1 direction.

2.1. Formulation of the dispersion equation

In this research, we assumed that the FGM plates are made of two different materials, and the materials of top and bottom are denoted M1, M2, respectively. The properties of internal materials are gradually changed from M1 to M2. With respect to the FGM plates, the parameters at any depth can be expressed as ρ (x_2) and C_{IJ} (x_2). Hence, based on the assumption of small deformation and the absence of body forces, the wave equation, generalized constitutive relations and the displacement-strain relationship can be expressed as:

$$\begin{aligned} &\sigma_{ij,j} = \rho(x_2)\frac{\partial^2 u_i}{\partial t^2} && i, j \in (1, 2, 3)\\ &\sigma_{ij} = C_{ijkl}(x_2)\varepsilon_{kl} && i, j, k, l \in (1, 2, 3)\\ &\varepsilon_{kl} = \tfrac{1}{2}(u_{k,l} + u_{l,k}) && k, l \in (1, 2, 3) \end{aligned} \tag{1}$$

where the σ_{ij} and ε_{kl} represent the stress tensor and strain tensor in the Cartesian coordinates, respectively, and u_i are the displacement components.

In FGM plates, the stress and displacement components can be defined in state matrix form:

$$\begin{aligned} &\mathbf{u} = [u_1 \;\; u_2 \;\; u_3]e^{-\mathrm{j}[kx_1-\omega t]}\\ &\boldsymbol{\tau}_{\mathrm{i}} = [\sigma_{i1} \;\; \sigma_{i2} \;\; \sigma_{i3}]e^{-\mathrm{j}[kx_1-\omega t]} \end{aligned} \tag{2}$$

where the k and ω are the wavenumber and angular frequency, respectively. To keep the consistent of state matrix form, the governing field equation and constitutive relations in terms of displacement and stress vector can be rewritten as:

$$\frac{\partial}{\partial x_2}\boldsymbol{\tau}_2 = -\rho(x_2)\omega^2\mathbf{u} - \frac{\partial}{\partial x_1}\boldsymbol{\tau}_1 - \frac{\partial}{\partial x_3}\boldsymbol{\tau}_3 \tag{3}$$

and

$$\begin{aligned}\tau_1 &= [D_{11}]\frac{\partial \mathbf{u}}{\partial x_1} + [D_{12}]\frac{\partial \mathbf{u}}{\partial x_2} + [D_{13}]\frac{\partial \mathbf{u}}{\partial x_3}\\ \tau_2 &= [D_{21}]\frac{\partial \mathbf{u}}{\partial x_1} + [D_{22}]\frac{\partial \mathbf{u}}{\partial x_2} + [D_{23}]\frac{\partial \mathbf{u}}{\partial x_3}\\ \tau_3 &= [D_{31}]\frac{\partial \mathbf{u}}{\partial x_1} + [D_{32}]\frac{\partial \mathbf{u}}{\partial x_2} + [D_{33}]\frac{\partial \mathbf{u}}{\partial x_3}\end{aligned} \tag{4}$$

where $[D_{ij}]$ are the elastic constant matrix C_{IJ} (x_2), which is directly influenced by gradient characteristics. Obviously, Eq. (4) can be rearranged along x_1 and x_3 directions by removing the first-order derivatives of u with respect to x_2:

$$\tau_1 = [D_{11}]\frac{\partial \mathbf{u}}{\partial x_1} + [D_{13}]\frac{\partial \mathbf{u}}{\partial x_3} + [D_{12}][D_{22}]^{-1}\left(\tau_2 - [D_{21}]\frac{\partial \mathbf{u}}{\partial x_1} - [D_{23}]\frac{\partial \mathbf{u}}{\partial x_3}\right) \tag{5}$$

$$\tau_3 = [D_{31}]\frac{\partial \mathbf{u}}{\partial x_1} + [D_{33}]\frac{\partial \mathbf{u}}{\partial x_3} + [D_{32}][D_{22}]^{-1}\left(\tau_2 - [D_{21}]\frac{\partial \mathbf{u}}{\partial x_1} - [D_{23}]\frac{\partial \mathbf{u}}{\partial x_3}\right) \tag{6}$$

Likewise, the corresponding vector forms can be written in the following forms:

$$\tau_1 = \left[[D_{12}][D_{22}]^{-1} \;\; -[D_{12}][D_{22}]^{-1}\left([D_{21}]\tfrac{\partial}{\partial x_1} + [D_{23}]\tfrac{\partial}{\partial x_3}\right) + [D_{11}]\tfrac{\partial}{\partial x_1} + [D_{13}]\tfrac{\partial}{\partial x_3}\right]\begin{pmatrix}\tau_2\\ \mathbf{u}\end{pmatrix} \tag{7}$$

$$\tau_3 = \left[[D_{32}][D_{22}]^{-1} \;\; -[D_{32}][D_{22}]^{-1}\left([D_{21}]\tfrac{\partial}{\partial x_1} + [D_{23}]\tfrac{\partial}{\partial x_3}\right) + [D_{31}]\tfrac{\partial}{\partial x_1} + [D_{33}]\tfrac{\partial}{\partial x_3}\right]\begin{pmatrix}\tau_2\\ \mathbf{u}\end{pmatrix} \tag{8}$$

Substituting Eqs. (7) and (8) into Eq. (3) can derive the matrix form of the derivatives of stress in the x_2 direction:

$$\frac{\partial}{\partial x_2}\tau_2 = [\,jk[D_{12}][D_{22}]^{-1} \;\; -\rho\omega^2 - k^2[[D_{12}][D_{22}]^{-1}[D_{21}] - [D_{11}]]]\begin{pmatrix}\tau_2\\ \mathbf{u}\end{pmatrix} \tag{9}$$

Referring to the matrix form of displacement and stress in the above formula, the Eq. (4) can also be rewritten as:

$$\frac{\partial}{\partial x_2}\mathbf{u} = [([D_{22}](x_2))^{-1} \;\; jk([D_{22}](x_2))^{-1}([D_{21}](x_2))]\begin{pmatrix}\tau_2\\ \mathbf{u}\end{pmatrix} \tag{10}$$

Combining the Eqs. (9) and (10) can obtain the following equation with matrix form:

$$\frac{\partial}{\partial x_2}\begin{pmatrix}\tau_2\\ \mathbf{u}\end{pmatrix} = \begin{pmatrix}jk[D_{12}][D_{22}]^{-1} & -\rho\omega^2 - k^2[[D_{12}][D_{22}]^{-1}[D_{21}] - [D_{11}]]\\ ([D_{22}](x_2))^{-1} & jk([D_{22}](x_2))^{-1}([D_{21}](x_2))\end{pmatrix}\begin{pmatrix}\tau_2\\ \mathbf{u}\end{pmatrix} \tag{11}$$

Next, in order to achieve the simplified solution of Eq. (11), and the propagation characteristics of guided wave along the x_1 direction, the FGM plate should be considered as a whole. Thus, the form of a general solution can be compactly expressed as:

$$\eta = \tilde{\eta}e^{j(\omega t - kx_1)} \tag{12}$$

where the state vector shows $\tilde{\eta} = [u_1 \;\; u_2 \;\; u_3 \;\; \sigma_{21} \;\; \sigma_{22} \;\; \sigma_{23}]^T$. By far, the wave equation of FGM plate, Eq. (11), can be represented by the following differential equations:

$$\frac{\partial \eta}{\partial x_2} = \bar{\mathbf{M}}\eta \tag{13}$$

Obviously,

$$\bar{\mathbf{M}} = \begin{pmatrix}jk[D_{12}][D_{22}]^{-1} & -\rho\omega^2 - k^2[[D_{12}][D_{22}]^{-1}[D_{21}] - [D_{11}]]\\ ([D_{22}](x_2))^{-1} & jk([D_{22}](x_2))^{-1}([D_{21}](x_2))\end{pmatrix} \tag{14}$$

The simplified displacement and stress expression are taken into account by substituting the derivative of the second equation of Eq. (4) versus x_2 into Eq. (11), the dispersion equation can be rearranged as follows:

$$k^2[D_{11}]\mathbf{u} + jk\frac{\partial[D_{21}]}{\partial x_2}\mathbf{u} + jk\frac{\partial \mathbf{u}}{\partial x_2}([D_{12}] + [D_{21}]) - \frac{\partial \mathbf{u}}{\partial x_2}\frac{\partial[D_{22}]}{\partial x_2} - \rho(x_2)\omega^2\mathbf{u} - \frac{\partial^2 \mathbf{u}}{\partial x_2^2}[D_{22}] = 0 \tag{15}$$

As we can see, the above equation are second-order partial derivation equation, which is related to the unknown wavenumber k and the displacement $\mathbf{u}$.

Meanwhile, to reduce the quantity of the computation process, it is necessary to introduce the reference unit elastic constant C_0, unit density ρ_0 and relative wavenumber $k_0 = \omega\sqrt{\rho_0/C_0}$. If both sides of Eq. (15) are divided by the square of reference wavenumber k_0, it can be written as:

$$\xi^2\frac{[D_{11}]\mathbf{u}}{C_0} + j\xi\frac{([D_{21}])'\mathbf{u}}{k_0C_0} + j\xi\frac{\partial \mathbf{u}}{\partial x_2}\frac{([D_{12}] + [D_{21}])}{k_0C_0} - \frac{\partial \mathbf{u}}{\partial x_2}\frac{([D_{22}])'}{k_0^2C_0} - \frac{\rho(x_2)}{\rho_0}\mathbf{u} - \frac{\partial^2 \mathbf{u}}{\partial x_2^2}\frac{[D_{22}]}{k_0^2C_0} = 0 \tag{16}$$

where $\xi = k/k_0$ is the normalized wavenumber, and $[D_{ij}]'$ are the first order derivatives of C_{IJ} (x_2) versus x_2 in Cartesian coordinate system.

2.2. Dispersion equations by Legendre polynomials

According to the principle of Galerkin method, we adopt the Legendre polynomial series as an orthogonal basis function in order to realize the superposition fitting of displacement field. Then, the displacement vector should be:

$$u_i = \sum_{n=0}^{N-1} U_n^i P_n(\chi) \tag{17}$$

where the $P_n(\chi)$ is the n^{th}-order Legendre polynomial, U_n^i represents the expansion coefficients of the amplitudes of the three displacement components $U^1(x_2)$, $U^2(x_2)$, $U^3(x_2)$. And N is the cut-off order of the selected Legendre polynomial series. Theoretically, the order of the Legendre series ranges from 0 to infinity, but the effective convergence can be achieved when the cut-off order approaches an enough big number M in practice, and the higher order terms can be effectively neglected. Since χ belongs to $[-1, 1]$, and the subdomain along the thickness direction x_2 is [0, h]. We should move x_2 into the range where the Legendre polynomial works, as:

$$\chi = \ell\left(x_2 - \frac{h}{2}\right), \quad \ell = 2/h \tag{18}$$

Submitting the Eqs. (17) and (18) into Eq. (16), and multiplying both sides of Eq. (16) by m^{th}-order Legendre polynomials, in which the m ranges from 0 to $M-1$. Then, integrate χ from -1 to 1. The linear equation system composed of $3M$ equations can be obtained theoretically, as:

$$\begin{aligned}&\xi^2\tfrac{[D_{11}]}{C_0}\textstyle\sum_{n=0}^{N-1}U_n^i\int_{-1}^{1}P_n(\chi)P_m(\chi)d\chi + j\xi\tfrac{([D_{21}])'}{\zeta_0C_0}\sum_{n=0}^{N-1}U_n^i\int_{-1}^{1}P_n(\chi)P_m(\chi)d\chi\\ &+ j\xi\ell\tfrac{([D_{12}]+[D_{21}])}{\zeta_0C_0}\textstyle\sum_{n=0}^{N-1}\int_{-1}^{1}\frac{\partial P_n(\chi)}{\partial\chi}P_m(\chi)d\chi\\ &- l\tfrac{([D_{22}])'}{\zeta_0^2C_0}\textstyle\sum_{n=0}^{N-1}\int_{-1}^{1}\frac{\partial P_n(\chi)}{\partial\chi}P_m(\chi)d\chi - \frac{\rho(x_2)}{\rho_0}\sum_{n=0}^{N-1}U_n^i\int_{-1}^{1}P_n(\chi)P_m(\chi)d\chi\\ &- \tfrac{[D_{22}]}{\zeta_0^2C_0}\ell^2\textstyle\sum_{n=0}^{N-1}\int_{-1}^{1}\frac{\partial^2P_n(\chi)}{\partial\chi^2}P_m(\chi)d\chi = 0\end{aligned} \tag{19}$$

The Voigt-type model [31] is used to calculate the effective material parameters of the FGM plates. Hence, the properties of the gradient material are described by:

$$\begin{aligned}C_{IJ}(x_2) &= C_{IJ}^2 + (C_{IJ}^1 - C_{IJ}^2)V_1(x_2)\\ \rho(x_2) &= \rho^2 + (\rho^1 - \rho^2)V_1(x_2)\end{aligned} \tag{20}$$

where $V_1(x_2)$ denotes the volume fraction of the surface material (which is pure M1), and $V_1(x_2) + V_2(x_2) = 1$. Moreover, the gradient

shape of the volume fraction can be expressed as a power series, exponential function and so on. We take Eq. (21) as an example here:

$$V_1 = \left(1 - \frac{x_2}{h}\right)^p \quad (0 \leqslant x_2 \leqslant h,\ 0.2 \leqslant p \leqslant 15) \tag{21}$$

where the exponential p determines the gradient shape of the FGM plate.

Because of the constraint of the orthogonal interval, the structural gradient model can be written as:

$$\begin{aligned} C_{IJ}(\chi) &= C_{IJ}^2 + (C_{IJ}^1 - C_{IJ}^2)\left(\frac{1}{2} - \frac{\chi}{2}\right)^p \\ \rho(x_2) &= \rho^2 + (\rho^1 - \rho^2)V_1 \\ C'_{IJ}(\chi) &= -\frac{p}{h}(C_{IJ}^1 - C_{IJ}^2)\frac{1}{2^{p-1}}(1-\chi)^{p-1} \end{aligned} \tag{22}$$

In our research, in order to make full use of the recursive property of Legendre polynomial series, the power function in the above equation can be fitted with the univariate nonlinear regression, as:

$$\begin{aligned} \left(\frac{1}{2} - \frac{\chi}{2}\right)^p &= S_1x^8 + S_2x^7 + S_3x^6 + S_4x^5 + S_5x^4 + S_6x^3 + S_7x^2 + S_8x^1 + S_9, \\ \left(\frac{1}{2} - \frac{\chi}{2}\right)^{p-1} &= Q_1x^8 + Q_2x^7 + Q_3x^6 + Q_4x^5 + Q_5x^4 + Q_6x^3 + Q_7x^2 + Q_8x^1 + Q_9; \end{aligned} \tag{23}$$

where the coefficients S_i and Q_i (i = 1,2,$\cdots$,9) can be determined by the Mathematica function 'Fit' [20] or MATLAB program 'curve Fiting'. Afterwards, submitting Eqs. (22) and (23) into Eq. (19), the dispersion equation can be finally obtained:

$$\begin{aligned} &\xi^2\frac{[D_{11}^2]}{C_0}\sum_{n=0}^{N-1}U_n^i\int_{-1}^{1}P_n(\chi)P_m(\chi)d\chi + j\xi\frac{([D_{12}^2]+[D_{21}^2])}{k_0C_0}l\sum_{n=0}^{N-1}\int_{-1}^{1}\frac{\partial P_n(\chi)}{\partial\chi}P_m(\chi)d\chi \\ &\quad - \rho_2\omega^2\sum_{n=0}^{N-1}U_n^i\int_{-1}^{1}P_n(\chi)P_m(\chi)d\chi \\ &- \frac{[D_{22}^2]}{k_0^2C_0}l^2\sum_{n=0}^{N-1}\int_{-1}^{1}\frac{\partial^2P_n(\chi)}{\partial\chi^2}P_m(\chi)d\chi \\ &\quad + \xi^2\frac{([D_{11}^1]-[D_{11}^2])}{C_0}\left(\begin{matrix}S_1x^8 + S_2x^7 + S_3x^6 + S_4x^5 + S_5x^4 \\ +S_6x^3 + S_7x^2 + S_8x^1 + S_9\end{matrix}\right)\sum_{n=0}^{N-1}U_n^i\int_{-1}^{1}P_n(\chi)P_m(\chi)d\chi \\ &- j\xi\frac{([D_{21}^1]-[D_{21}^2])}{k_0C_0}\frac{p}{h}(Q_1x^8 + Q_2x^7 + Q_3x^6 + Q_4x^5 + Q_5x^4 + Q_6x^3 + Q_7x^2 + Q_8x^1 \\ &\quad + Q_9)\sum_{n=0}^{N-1}U_n^i\int_{-1}^{1}P_n(\chi)P_m(\chi)d\chi \\ &+ j\xi\ell\frac{(([D_{12}^1]-[D_{12}^2])+([D_{21}^1]-[D_{21}^2]))}{k_0C_0}\left(\begin{matrix}S_1x^8 + S_2x^7 + S_3x^6 + S_4x^5 + S_5x^4 \\ +S_6x^3 + S_7x^2 + S_8x^1 + S_9\end{matrix}\right)\sum_{n=0}^{N-1}\int_{-1}^{1}\frac{\partial P_n(\chi)}{\partial\chi}P_m \\ &\quad (\chi)d\chi \\ &+ l\frac{([D_{22}^1]-[D_{22}^2])}{k_0^2C_0}\frac{p}{h}(Q_1x^8 + Q_2x^7 + Q_3x^6 + Q_4x^5 + Q_5x^4 + Q_6x^3 + Q_7x^2 + Q_8x^1 \\ &\quad + Q_9)\sum_{n=0}^{N-1}\int_{-1}^{1}\frac{\partial P_n(\chi)}{\partial\chi}P_m(\chi)d\chi \\ &- \frac{(\rho_1-\rho_2)}{\rho_0}(S_1x^8 + S_2x^7 + S_3x^6 + S_4x^5 + S_5x^4 + S_6x^3 + S_7x^2 + S_8x^1 \\ &\quad + S_9)\sum_{n=0}^{N-1}U_n^i\int_{-1}^{1}P_n(\chi)P_m(\chi)d\chi \\ &- \frac{([D_{22}^1]-[D_{22}^2])}{k_0^2C_0}\ell^2(S_1x^8 + S_2x^7 + S_3x^6 + S_4x^5 + S_5x^4 + S_6x^3 + S_7x^2 + S_8x^1 \\ &\quad + S_9)\sum_{n=0}^{N-1}\int_{-1}^{1}\frac{\partial^2P_n(\chi)}{\partial\chi^2}P_m(\chi)d\chi = 0 \end{aligned} \tag{24}$$

where $\frac{\partial P_n(\chi)}{\partial\chi}$, $\frac{\partial^2P_n(\chi)}{\partial\chi^2}$, $x^qP_n(\chi)$, $x^q\frac{\partial P_n(\chi)}{\partial\chi}$, $x^q\frac{\partial^2P_n(\chi)}{\partial\chi^2}$ (q = 1, 2, … 8) are the linear operators associated with the Legendre polynomial, totally 26 terms, as shown in Appendix A in details. In order to avoid the complicated integral operation in the dispersion equations, the analytical expression of the above linear operator can be obtained through the orthogonal completeness and strong recursive property of Legendre polynomial series. This will improve the computational efficiency significantly. As a matter of fact, Eq. (24) can only provide $3(M-2)$ equations, which is difficult to satisfy the theoretical solution of $3M$ unknownsU_n^i. So, applying the traction-free on the surface of the FGM plate, the corresponding boundary conditions are introduced:

Boundary conditions

$$\begin{cases} \sum_{n=0}^{N}\left(-j\xi[D_{21}^2] + \frac{[D_{22}^2]}{k_0}\ell\frac{n(n+1)}{2}\right)U_n = 0 & \text{(upper)} \\ \sum_{n=0}^{N}\left(-(-1)^nj\xi[D_{21}^1] + \frac{[D_{22}^1]}{k_0}(-1)^{n+1}\ell\frac{n(n+1)}{2}\right)U_n & \text{(lower)} \\ \quad = 0 \end{cases} \tag{25}$$

Combing the Eq. (24) and Eq. (25), the linear equation system can be written as:

$$\xi^2\mathbf{\Gamma}_{3N\times3N}\mathbf{E}_{3N\times1} + j\xi\mathbf{\Psi}_{3N\times3N}\mathbf{D}_{3N\times1} + \mathbf{Z}_{3N\times3N}\mathbf{D}_{3N\times1} = 0 \tag{26}$$

where $\mathbf{\Gamma}_{3N\times3N}$, $\mathbf{\Psi}^k_{3N\times3N}$, $\mathbf{Z}_{3N\times3N}$ are the corresponding coefficient matrices, and $\mathbf{E}_i = [U_0^i, U_1^i, \ldots U_{N-1}^i]^T$. In order to solve the above quadratic eigenvalue problem, we introduce the unit matrix $\mathbf{I}$ and auxiliary variable $\mathbf{R}_{3N\times1} = j\xi\mathbf{\Gamma}_{3N\times3N}\mathbf{E}_{3N\times1}$ to modify the Eq. (26), as:

$$\left(\begin{bmatrix}\mathbf{\Psi}_{3N\times3N} & -I_{3N\times3N} \\ -\mathbf{\Gamma}_{3N\times3N} & 0\end{bmatrix} - \frac{j}{\xi}\begin{bmatrix}\mathbf{Z}_{3N\times3N} & 0 \\ 0 & I_{3N\times3N}\end{bmatrix}\right)\begin{bmatrix}\mathbf{E}_{3N\times1} \\ \mathbf{R}_{3N\times1}\end{bmatrix} = 0 \tag{27}$$

Finally, we note that the eigenvalue problem can be solved by using the MATLAB 'eig' function (employ the QZ algorithm) when the wavenumber varies. The phase velocity can be obtained by $\omega = c\xi$ (eigenvalues), and eigenvectors $\mathbf{E}$ can be used to describe the wave profile. So, it can be seen that dispersion curves, displacement and stress distribution of FGM plates can be acquired effectively at the same time by this proposed method. It should be noted that the matrices in the final governing equations appear in the form of triangular matrix and are highly symmetrical by introducing the state vector $\boldsymbol{\eta}$, which maximizes the computation efficiency of matrix operations.

3. Numerical results and discussion

3.1. Validation

Based on the pervious formulations, a computational program in terms of the State-vector formalism and Legendre polynomial (SVFLP) method is developed by MATLAB, which is conducted to calculate the dispersion curves of guided waves propagation in the FGM plates with different gradient shape. Firstly, in order to verify the validity of the programming and theoretical formulas, we calculate the Cr-ceramics FGM plate with two different gradient index p to make a comparison between our results with the available data [23], as shown in Fig. 2. The mechanical parameters used can also be found in Ref. [23]. It should be noted that, Fig. 2(a) is the dispersion curves from the power series technique, and Fig. 2(b) is the numerical results by the proposed SVFLP method. The cut-off order of the Legendre orthogonal polynomial series is M = 15. The red dot line and bule dot line in Fig. 2(b) represent results with the p = 1, 10, respectively. In the range of $kh \leq 10$, it clearly shows that the numerical solutions by SVFLP method are consistent with the results obtained by power series technique, which validates that our proposed method is effective in solving wave propagation problems of FGM plates.

3.2. Guided wave propagation characteristics in FGM plate

Iron based alumina FGM plate with thickness of 1 mm is studied here. The surface, at $x_2 = 0$, is homogeneous Fe-rich, while at $x_2 = h$, it's aluminum oxide-rich. The material parameters are given in Table 1. Meanwhile, mechanical properties at arbitrary position along thickness direction in FGM plate can be obtained via Eq. (20). Here, we assumed that the gradient index p were equal to 0.2, 0.5, 1, 2, 10, 15. It can be clearly seen that, in Fig. 3, gradient exponents significantly changed the variation trend of volume fraction distribution along thickness direction. As the increase of gradient index p, the proportion of alumina in the FGM plate also increases; when the gradient exponent approaches infinity, the content of Fe approximately goes to zero. So, different

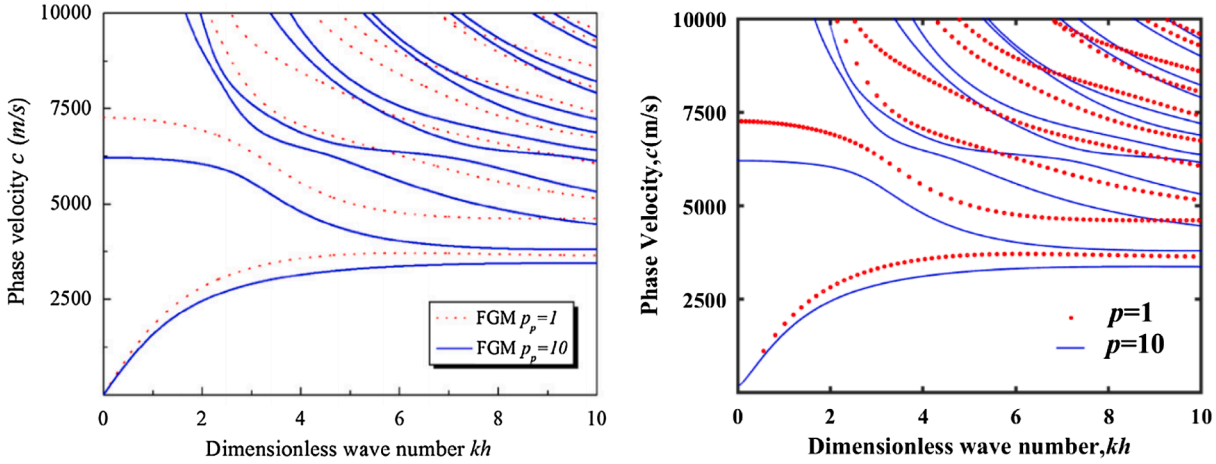

(a) The results from Ref. [23] (b) The results by SVFLP method

Fig. 2. Dispersion curves of Lamb waves for Cr-ceramics FGM plate.

gradient fields result in different volume fractions by varying different gradient exponents.

To illustrate the effect of gradient field on the wave propagation characteristics, we calculated the corresponding dispersion curves in the Iron based alumina FGM plate when p = 0.2, 0.5, 1, 2, 10, 15, respectively, as shown in Fig. 4(a–f). The results show that the gradient field can influence the elastic modes significantly in the range of 0–8 MHz. We can find out from these figures that the overall trend gradually tends to the Al_2O_3 material, while p increases. And the dispersive phenomenon of SH_0 mode seems to be more and more apparent in this frequency range. Also, the phase velocities of foundation modes, A_0, S_0, increase with p at zero frequency. Interestingly, as a typical two-phase functionally gradient material, the convergence value of A_0 and S_0 modes are not close enough to a steady value as the frequency increases, even when the frequency thickness product goes to 8 MHz mm. In contrast, it is worth noting that the phase velocities of S_0 and A_0 in homogeneous isotropic plate gradually approach the Rayleigh wave velocity.

3.3. Convergence of the problem

Different from traditional matrix method and power series method, the propagation characteristics can be determined by turning the transcendental equation into an non-iterative eigenvalue problem through the proposed method. The common starting point of solving the wave problem is viewing the displacement as a general solution form. In this method, the displacement solution is fitted approximately by the Legendre polynomial within a finite number of terms, which is the so called cut-off order M. It will directly affects the accuracy and stability of the calculation results. To validate the convergence of the proposed method, the guided wave dispersion curves of Iron based alumina FGM plate are calculated at p = 1 versus different cut-off orders M = 8, 9, 10, 11, respectively. As shown in Fig. 5, Fig. 5(a) shows that it seems all the modes converge in the range of 0–6 MHz, when $M \geq 8$. However, the calculation results are not much consistent with each other in 6–8 MHz. If we take a look at the local part, as shown in Fig. 5(b), it can be concluded that different dispersion curves corresponding to each cut-off order are gradually approaching to each other, when M increases. Obviously, the agreement is quite good between the results from M = 10 and M = 11. Thus, good convergence in the range of 0–8 MHz can be observed when the cut-off order $M \geq 10$. Generally, the larger cut off order N is, the more the convergent and stable of the numerical results will be. Hence, we take M = 12 in the above example, as shown in Fig. 4.

Table 1
Mechanical properties of Fe-Al_2O_3 material [32].

Materials	ρ (kg/m^3)	C_{11} (GPa)	C_{12} (GPa)	C_{44} (GPa)
Fe	7870	218.5	63.6	77.5
Al_2O_3	3900	388.8	85.5	140.0

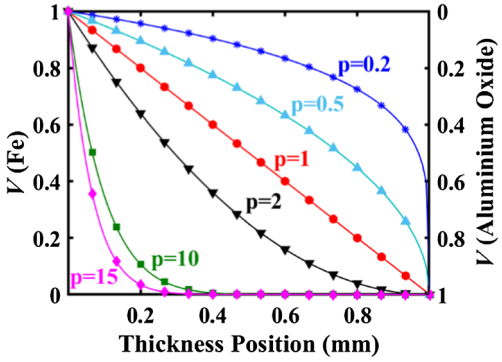

Fig. 3. Variation curves of the volume fraction in Iron based alumina FGM plate.

3.4. Stress distributions

In order to investigate the wave propagation characteristics in details, we discuss the stress distributions of the Iron based alumina FGM plate with different p at a given frequency. As shown in Fig. 6, considering a given point in S_0 mode at f = 1 MHz with different gradient shapes, its corresponding stress profile can be obtained according to the eigenvector $\mathbf{E}$ combining Eq. (4). These figures are displayed in normalized axis. It can be observed that on the top and bottom surfaces of the FGM plate, the direct stress σ_{22} and the shear stress σ_{21}, σ_{23} are zero in the arbitrary gradient field, which is consistent with the boundary conditions. In addition, the effect of gradient field on the stress distributions shows that the amplitude of relative σ_{22} declines significantly with the increase of the gradient index p. Similarly, it can be seen that the peak amplitude of stress component σ_{21} shifts gradually downward in the thickness direction. Moreover, the continuous distributions of stress field along the thickness direction can be also used to verify the

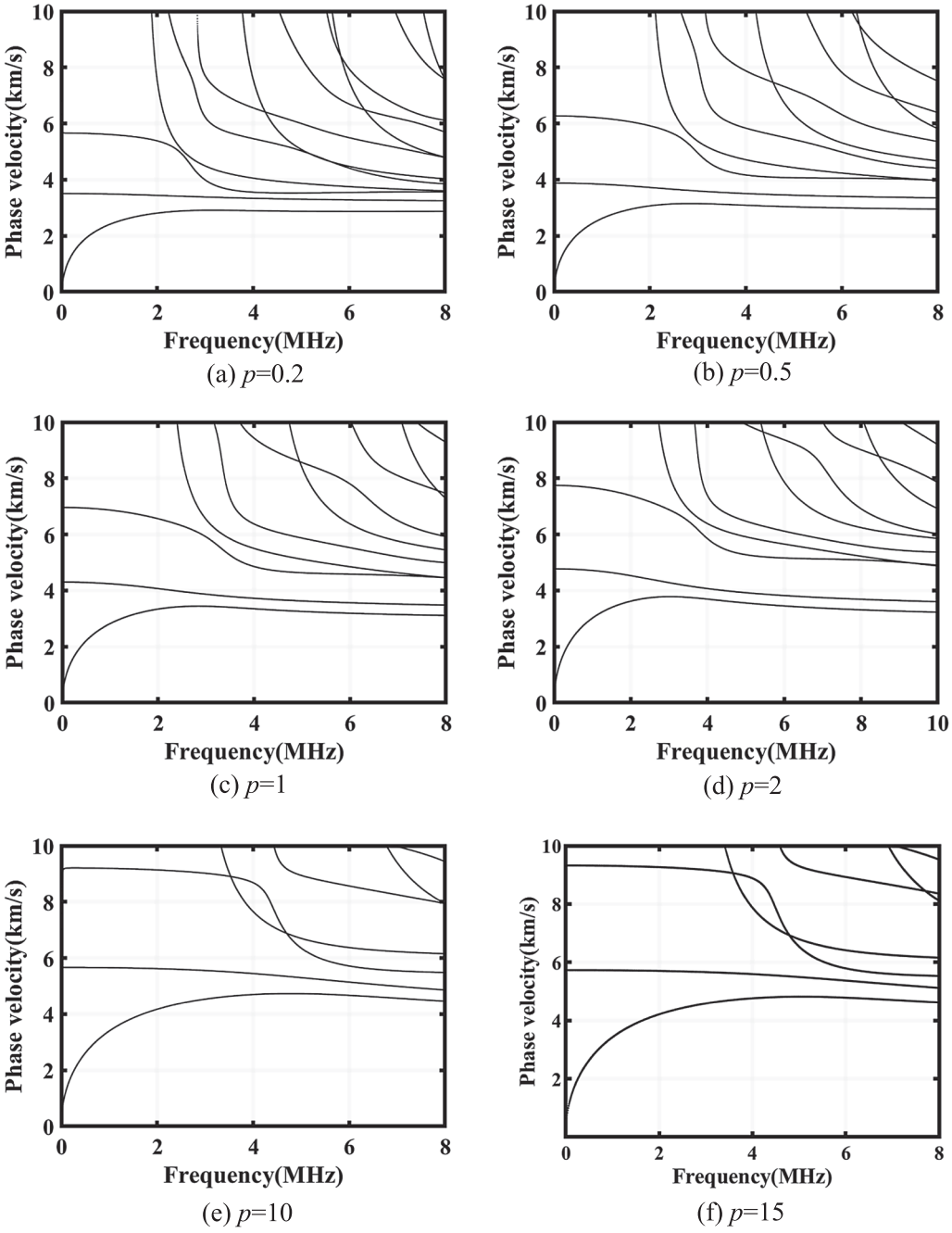

Fig. 4. Dispersion curves of guided waves propagation in Fe-Al_2O_3 FGM plate with different p.

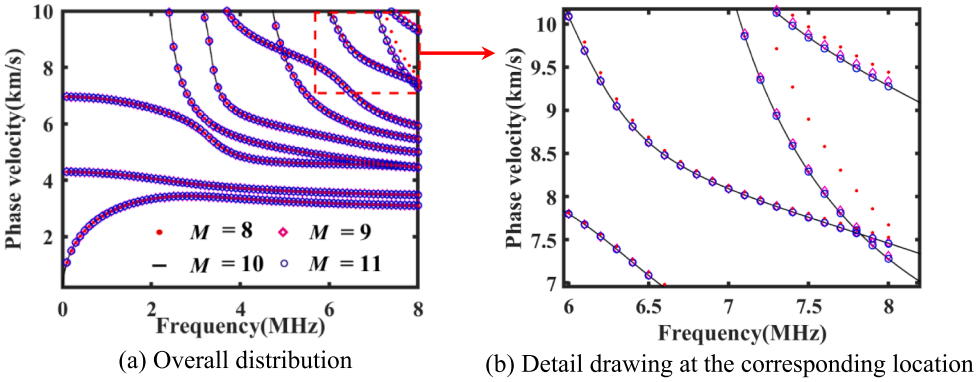

Fig. 5. Dispersion curves of propagating guided wave in FGM plate with various cut-off order M.

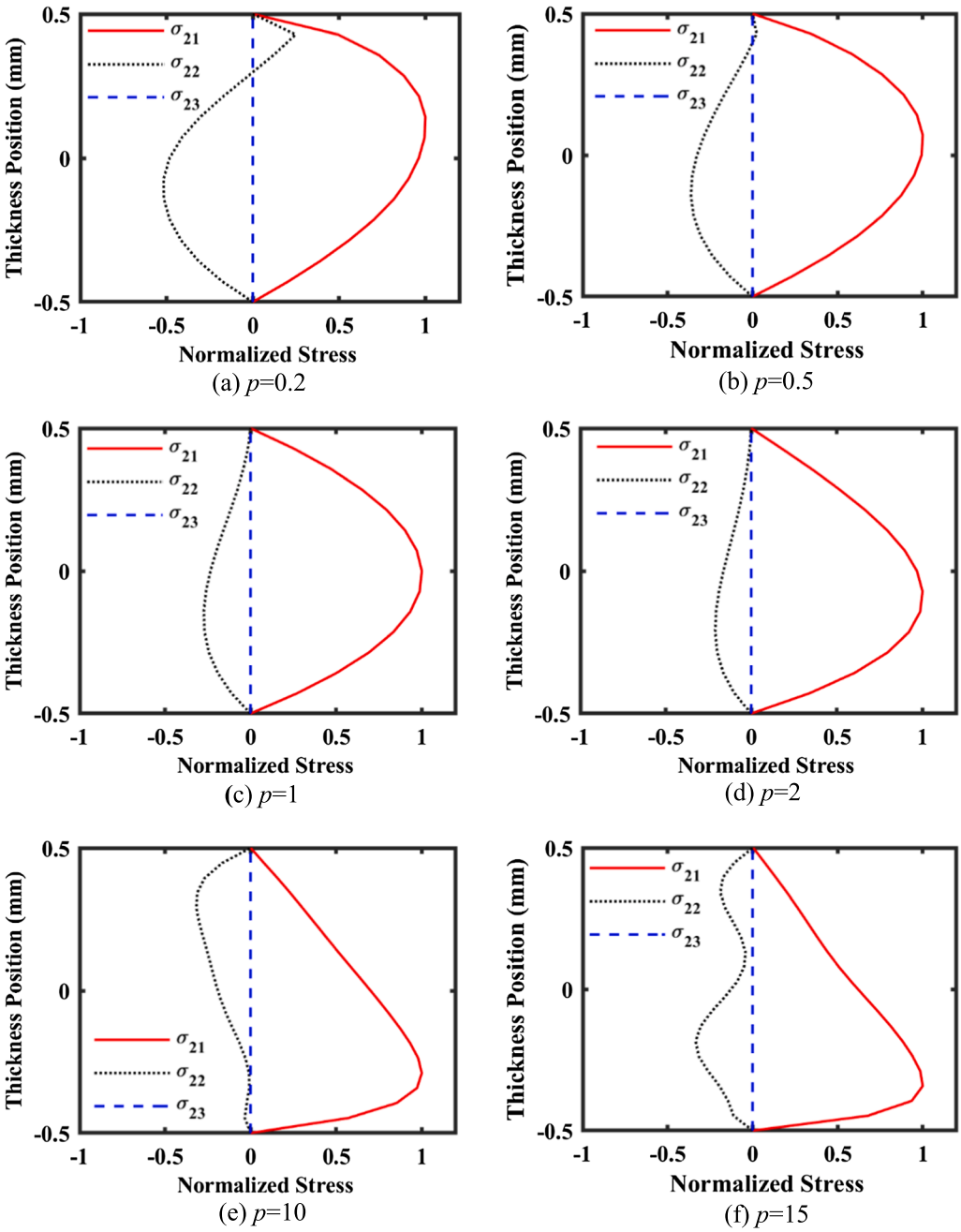

Fig. 6. Stress distributions in Fe-Al_2O_3 FGM plate with different *p*.

feasibility and correctness of the SVFLP method for the computation of the dispersion curves in the FGM plates.

4. Conclusions

The aim of this research was to propose an analytical method to calculate the wave propagation problem in continuous FGM plate without discretizing the gradient structure into homogeneous multi-layered model. Based on the State-vector formalism and Legendre polynomial (SVFLP) method, the propagation characteristics of guided waves in FGM plates with continuous changes in mechanical properties (density, elastic constants) along the thickness direction can be obtained effectively. Meanwhile, this method is verified by comparing with the earlier results. Then, the propagation of guided waves in Fe-Al_2O_3 FGM plates has been investigated, and the numerical results show that the gradient field possesses obvious influence both on dispersion curves and stress distributions. We also analyze the effect of different Legendre polynomial cut-off order *M* on the convergence of the elastic modes in the range of 0–8 MHz. Moreover, the relationship between the gradient distribution and propagation characteristics can be established

by SVFLP, which provides theoretical guideline for quantitative inversion of the elastic properties of FGM plates. This may encourage one to go further to access multiple physical field coupling on acoustic propagation characteristics in FGM.

Author contribution

The research was raised by Jie Gao, Yan Lyu and other co-authors. And the research work was also conducted by Gao and Lyu, who played a major part in the development of the method mentioned in this manuscript. Gao and Lyu carried out the theoretical derivation, developed the relative programs, together with the main writing of this manuscript. Mingfang Zheng and Mingkun Liu put forward many constructive suggestions for the development of the approach, and inspected the results of theoretical calculations. Hongye Liu, Bin Wu and Cunfu He joined the discussion for the development of the method, and offered some useful proposals.

Acknowledgments

This work is supported by national Natural Science Foundation of China (Nos. 51505013, 11872082, 11527801).

Appendix A

The linear operators of the Legendre polynomials series in Eq. (24) can be described as $\frac{\partial P_n(\chi)}{\partial \chi}$, $\frac{\partial^2 P_n(\chi)}{\partial \chi^2}$, $x^q P_n(\chi)$, $x^q \frac{\partial P_n(\chi)}{\partial \chi}$, $x^q \frac{\partial^2 P_n(\chi)}{\partial \chi^2}$ by the recurrence relation. Here, the expressions of the $\frac{\partial P_n(\chi)}{\partial \chi}$ and $\frac{\partial^2 P_n(\chi)}{\partial \chi^2}$ are as follows in Eq. (A-1):

$$\begin{aligned}
&\frac{\partial u}{\partial \chi} = \sum_{n=0}^{N-1} \Psi_l^n \frac{\partial P_n(\chi)}{\partial \chi} = \sum_{n=0}^{N-2} q_l{}^n P_n(\chi) \\
&\frac{\partial^2 u}{\partial \chi^2} = \sum_{n=0}^{N-1} \Psi_l^n \frac{\partial^2 P_n(\chi)}{\partial \chi^2} = \sum_{n=0}^{N-3} p_l{}^n P_n(\chi)
\end{aligned} \tag{A-1}$$

where

$$\begin{aligned}
&q_l{}^m = (2m+1) \sum_{n=m+1,m+3,\cdots}^{N-1} \Psi_l^n \\
&p_l{}^m = \left(\frac{2m+1}{2}\right) \sum_{n=m+2,m+4,\cdots}^{N-1} (n(n+1) - m(m+1)) \Psi_l^n
\end{aligned}$$

Likewise, the elements of $x^q P_n(\chi)$ can be written as Eq. (A-2):

$$\begin{aligned}
&\chi u = \sum_{n=0}^{N-1} \Psi_l^n \chi P_n(\chi) = \sum_{n=0}^{N-2} A_l{}^n P_n(\chi) \\
&\chi^2 u = \sum_{n=0}^{N-1} \Psi_l^n \chi^2 P_n(\chi) = \sum_{n=0}^{N-2} B_l{}^n P_n(\chi) \\
&\chi^3 u = \sum_{n=0}^{N-1} \Psi_l^n \chi^3 P_n(\chi) = \sum_{n=0}^{N-2} C_l{}^n P_n(\chi) \\
&\chi^4 u = \sum_{n=0}^{N-1} \Psi_l^n \chi^4 P_n(\chi) = \sum_{n=0}^{N-2} D_l{}^n Q_n(\chi) \\
&\chi^5 u = \sum_{n=0}^{N-1} \Psi_l^n \chi^5 P_n(\chi) = \sum_{n=0}^{N-2} E_l{}^n P_n(\chi) \\
&\chi^6 u = \sum_{n=0}^{N-1} \Psi_l^n \chi^6 P_n(\chi) = \sum_{n=0}^{N-2} F_l{}^n P_n(\chi) \\
&\chi^7 u = \sum_{n=0}^{N-1} \Psi_l^n \chi^7 P_n(\chi) = \sum_{n=0}^{N-2} G_l{}^n P_n(\chi) \\
&\chi^8 u = \sum_{n=0}^{N-1} \Psi_l^n \chi^8 P_n(\chi) = \sum_{n=0}^{N-2} H_l{}^n P_n(\chi)
\end{aligned} \tag{A-2}$$

where

$$A_l{}^m = \frac{m}{(2m-1)} \Psi_l^{m-1} + \frac{m+1}{(2m+3)} \Psi_l^{m+1}$$

$$B_l^n = \frac{(n+1)(n+2)}{(2n+1)(2n+3)} \Psi_l^{n+2} + J \Psi_l^n + \frac{n(n-1)}{(2n+1)(2n-1)} \Psi_l^{n-2}$$

$$C_l^n = \frac{(n+1)(n+2)(n+3)}{(2n+1)(2n+3)(2n+5)} \Psi_l^{n+3} + K_1 \Psi_l^{n+1} + L_1 \Psi_l^{n-1} + \frac{n(n-1)(n-2)}{(2n+1)(2n-1)(2n-3)} \Psi_l^{n-3}$$

$$D_l^n = \frac{(n+1)(n+2)(n+3)(n+4)}{(2n+1)(2n+3)(2n+5)(2n+7)} \Psi_l^{n+4} + K_2 \Psi_l^{n+2} + L_2 \Psi_l^n + M_2 \Psi_l^{n-2} + \frac{n(n-1)(n-2)(n-3)}{(2n+1)(2n-1)(2n-3)(2n-5)} \Psi_l^{n-4}$$

$$E_l^n = \frac{(n+1)(n+2)(n+3)(n+4)(n+5)}{(2n+1)(2n+3)(2n+5)(2n+7)(2n+9)} \Psi_l^{n+5} + K_3 \Psi_l^{n+3} + L_3 \Psi_l^{n+1} + M_3 \Psi_l^{n-1} + N_3 \Psi_l^{n-3} + \frac{n(n-1)(n-2)(n-3)(n-4)}{(2n+1)(2n-1)(2n-3)(2n-5)(2n-7)} \Psi_l^{n-5}$$

$$F_l^n = \frac{(n+1)(n+2)(n+3)(n+4)(n+5)(n+6)}{(2n+1)(2n+3)(2n+5)(2n+7)(2n+9)(2n+11)} \Psi_l^{n+6} + K_4 \Psi_l^{n+4} + L_4 \Psi_l^{n+2} + M_4 \Psi_l^n + N_4 \Psi_l^{n-2} + P_4 \Psi_l^{n-4} + \frac{n(n-1)(n-2)(n-3)(n-4)(n-5)}{(2n+1)(2n-1)(2n-3)(2n-5)(2n-7)(2n-9)} \Psi_l^{n-6}$$

$$G_l^n = \frac{(n+1)(n+2)(n+3)(n+4)(n+5)(n+6)(n+7)}{(2n+1)(2n+3)(2n+5)(2n+7)(2n+9)(2n+11)(2n+13)} \Psi_l^{n+7} + K_5 \Psi_l^{n+5} + L_5 \Psi_l^{n+3} + M_5 \Psi_l^{n+1} + N_5 \Psi_l^{n-1} + P_5 \Psi_l^{n-3} + Q_5 \Psi_l^{n-5} + \frac{n(n-1)(n-2)(n-3)(n-4)(n-5)(n-6)}{(2n+1)(2n-1)(2n-3)(2n-5)(2n-7)(2n-9)(2n-11)} \Psi_l^{n-7}$$

$$H_l^n = \frac{(n+1)(n+2)(n+3)(n+4)(n+5)(n+6)(n+7)(n+8)}{(2n+1)(2n+3)(2n+5)(2n+7)(2n+9)(2n+11)(2n+13)(2n+15)} \Psi_l^{n+8} + K_6 \Psi_l^{n+6} + L_6 \Psi_l^{n+4} + M_6 \Psi_l^{n+2} + N_6 \Psi_l^n + P_6 \Psi_l^{n-2} + Q_6 \Psi_l^{n-4} + R_6 \Psi_l^{n-6} + \frac{n(n-1)(n-2)(n-3)(n-4)(n-5)(n-6)(n-7)}{(2n+1)(2n-1)(2n-3)(2n-5)(2n-7)(2n-9)(2n-11)(2n-13)} \Psi_l^{n-8}$$

$$J = \left[\frac{(n+1)^2}{(2n+3)(2n+1)} + \frac{(n)^2}{(2n+1)(2n-1)}\right]$$
$$K_1 = \left[\frac{(n+1)(n+2)^2}{(2n+1)(2n+3)(2n+5)} + \frac{(n+1)J}{(2n+1)}\right]$$
$$L_1 = \left[\frac{(n)J}{(2n+1)} + \frac{n(n-1)^2}{(2n+1)(2n-1)(2n-3)}\right]$$
$$K_2 = \left[\frac{(n+1)(n+2)(n+3)^2}{(2n+1)(2n+3)(2n+5)(2n+7)} + \frac{(n+2)K_1}{2n+3}\right]$$
$$L_2 = \left[\frac{(n+1)K_1}{2n+3} + \frac{nL_1}{2n-1}\right]$$
$$M_2 = \left[\frac{(n-1)L_1}{2n-1} + \frac{n(n-1)(n-2)^2}{(2n+1)(2n-1)(2n-3)(2n-5)}\right]$$
$$K_3 = \left[\frac{(n+1)(n+2)(n+3)(n+4)^2}{(2n+1)(2n+3)(2n+5)(2n+7)(2n+9)} + \frac{(n+3)K_2}{2n+5}\right]$$
$$L_3 = \left[\frac{(n+2)K_2}{2n+5} + \frac{(n+1)L_2}{2n+1}\right]$$
$$M_3 = \left[\frac{nL_2}{2n+1} + \frac{(n-1)M_2}{2n-3}\right]$$
$$N_3 = \left[\frac{(n-2)M_2}{2n-3} + \frac{n(n-1)(n-2)(n-3)^2}{(2n+1)(2n-1)(2n-3)(2n-5)(2n-7)}\right]$$
$$K_4 = \left[\frac{(n+1)(n+2)(n+3)(n+4)(n+5)^2}{(2n+1)(2n+3)(2n+5)(2n+7)(2n+9)(2n+11)} + \frac{(n+4)K_3}{2n+7}\right]$$
$$L_4 = \left[\frac{(n+3)K_3}{2n+7} + \frac{(n+2)L_3}{2n+3}\right]$$
$$M_4 = \left[\frac{(n+1)L_3}{2n+3} + \frac{nM_3}{2n-1}\right]$$
$$N_4 = \left[\frac{(n-1)M_3}{2n-1} + \frac{(n-2)N_3}{2n-5}\right]$$
$$L_5 = \left[\frac{(n+4)K_4}{2n+9} + \frac{(n+3)L_4}{2n+5}\right]$$
$$P_4 = \left[\frac{(n-3)N_3}{2n-5} + \frac{n(n-1)(n-2)(n-3)(n-4)^2}{(2n+1)(2n-1)(2n-3)(2n-5)(2n-7)(2n-9)}\right]$$
$$M_5 = \left[\frac{(n+2)L_4}{2n+5} + \frac{(n+1)M_4}{2n+1}\right]$$
$$K_5 = \left[\frac{(n+1)(n+2)(n+3)(n+4)(n+5)(n+6)^2}{(2n+1)(2n+3)(2n+5)(2n+7)(2n+9)(2n+11)(2n+13)} + \frac{(n+5)K_4}{2n+9}\right]$$
$$N_5 = \left[\frac{nM_4}{2n+1} + \frac{(n-1)N_4}{2n-3}\right]$$
$$P_5 = \left[\frac{(n-2)N_4}{2n-3} + \frac{(n-3)P_4}{2n-7}\right]$$

$$Q_5 = \left[\frac{(n-4)P_4}{2n-7} + \frac{n(n-1)(n-2)(n-3)(n-4)(n-5)^2}{(2n+1)(2n-1)(2n-3)(2n-5)(2n-7)(2n-9)(2n-11)}\right]$$
$$Q_6 = \left[\frac{(n-3)P_5}{2n-5} + \frac{(n-4)Q_5}{2n-9}\right]$$
$$L_6 = \left[\frac{(n+5)K_5}{2n+11} + \frac{(n+4)L_5}{2n+7}\right]$$
$$M_6 = \left[\frac{(n+3)L_5}{2n+7} + \frac{(n+2)M_5}{2n+3}\right]$$
$$N_6 = \left[\frac{(n+1)M_5}{2n+3} + \frac{nN_5}{2n-1}\right]$$
$$P_6 = \left[\frac{(n-1)N_5}{2n-1} + \frac{(n-2)P_5}{2n-5}\right]$$
$$K_6 = \left[\frac{(n+1)(n+2)(n+3)(n+4)(n+5)(n+6)(n+7)^2}{(2n+1)(2n+3)(2n+5)(2n+7)(2n+9)(2n+11)(2n+13)(2n+15)} + \frac{(n+6)K_5}{2n+11}\right]$$
$$R_6 = \left[\frac{(n-5)Q_5}{2n-9} + \frac{n(n-1)(n-2)(n-3)(n-4)(n-5)(n-6)^2}{(2n+1)(2n-1)(2n-3)(2n-5)(2n-7)(2n-9)(2n-11)(2n-13)}\right]$$

And the elements of $x^q\frac{\partial P_n(\chi)}{\partial \chi}$are given in Eq. (A-3):

$$\begin{aligned}
\chi\frac{\partial u}{\partial \chi} &= \sum_{n=0}^{N-1}\Psi_l^n\chi\frac{\partial P_n(\chi)}{\partial \chi} = \sum_{n=0}^{N-2} I_l^n P_n(\chi)\\
\chi^2\frac{\partial u}{\partial \chi} &= \sum_{n=0}^{N-1}\Psi_l^n\chi^2\frac{\partial P_n(\chi)}{\partial \chi} = \sum_{n=0}^{N-2} J_l^n P_n(\chi)\\
\chi^3\frac{\partial u}{\partial \chi} &= \sum_{n=0}^{N-1}\Psi_l^n\chi^3\frac{\partial P_n(\chi)}{\partial \chi} = \sum_{n=0}^{N-2} K_l^n P_n(\chi)\\
\chi^4\frac{\partial u}{\partial \chi} &= \sum_{n=0}^{N-1}\Psi_l^n\chi^4\frac{\partial P_n(\chi)}{\partial \chi} = \sum_{n=0}^{N-2} L_l^n P_n(\chi)\\
\chi^5\frac{\partial u}{\partial \chi} &= \sum_{n=0}^{N-1}\Psi_l^n\chi^5\frac{\partial P_n(\chi)}{\partial \chi} = \sum_{n=0}^{N-2} M_l^n P_n(\chi)\\
\chi^6\frac{\partial u}{\partial \chi} &= \sum_{n=0}^{N-1}\Psi_l^n\chi^6\frac{\partial P_n(\chi)}{\partial \chi} = \sum_{n=0}^{N-2} N_l^n P_n(\chi)\\
\chi^7\frac{\partial u}{\partial \chi} &= \sum_{n=0}^{N-1}\Psi_l^n\chi^7\frac{\partial P_n(\chi)}{\partial \chi} = \sum_{n=0}^{N-2} O_l^n P_n(\chi)\\
\chi^8\frac{\partial u}{\partial \chi} &= \sum_{n=0}^{N-1}\Psi_l^n\chi^8\frac{\partial P_n(\chi)}{\partial \chi} = \sum_{n=0}^{N-2} P_l^n P_n(\chi)
\end{aligned} \tag{A-3}$$

where

$$I_l^m = m\Psi_l^m + (2m+1)\sum_{n=m+2,m+4,\cdots}^{N-1}\Psi_l^n$$

$$J_l^m = \frac{m(m-1)}{2m-1}\Psi_l^{m-1} + ((m+1)^2/(2m+3)+m)\Psi_l^{m+1} + (2m+1)\sum_{n=m+3,n=m+5,\cdots}^{N-1}\Psi_l^n$$

$$K_l^n = (2m+1)\sum_{n=m+4,\cdots}^{N-1}\Psi_l^n + U_1\Psi_l^{n-2} + V_1\Psi_l^n + \frac{n(n+1)(n+2)}{(2n+1)(2n+3)}\Psi_l^{n+2}$$

$$L_l^n = (2m+1)\sum_{n=m+5,\cdots}^{N-1}\Psi_l^n + U_2\Psi_l^{n+1} + V_2\Psi_l^{n-1} + W_2\Psi_l^{n-3} + \frac{n(n+1)(n+2)(n+3)}{(2n+1)(2n+3)(2n+5)}\Psi_l^{n+3}$$

$$M_l^n = (2m+1)\sum_{n=m+6,\cdots}^{N-1}\Psi_l^n + U_3\Psi_l^{n+2} + V_3\Psi_l^n + W_3\Psi_l^{n-2} + X_3\Psi_l^{n-4} + \frac{n(n+1)(n+2)(n+3)(n+4)}{(2n+1)(2n+3)(2n+5)(2n+7)}\Psi_l^{n+4}$$

$$N_l^n = (2m+1)\sum_{n=m+7,\cdots}^{N-1}\Psi_l^n + U_4\Psi_l^{n+3} + V_4\Psi_l^{n+1} + W_4\Psi_l^{n-1} + X_4\Psi_l^{n-3} + Y_4\Psi_l^{n-5} + \frac{n(n+1)(n+2)(n+3)(n+4)(n+5)}{(2n+1)(2n+3)(2n+5)(2n+7)(2n+9)}\Psi_l^{n+5}$$

$$O_l^n = (2m+1)\sum_{n=m+8,\cdots}^{N-1}\Psi_l^n + U_5\Psi_l^{n+4} + V_5\Psi_l^{n+2} + W_5\Psi_l^n + X_5\Psi_l^{n-2} + Y_5\Psi_l^{n-4} + Z_5\Psi_l^{n-6} + \frac{n(n+1)(n+2)(n+3)(n+4)(n+5)(n+6)}{(2n+1)(2n+3)(2n+5)(2n+7)(2n+9)(2n+11)}\Psi_l^{n+6}$$

$$P_l^n = (2m+1)\sum_{n=m+9,\cdots}^{N-1}\Psi_l^n + U_6\Psi_l^{n+5} + V_6\Psi_l^{n+3} + W_6\Psi_l^{n+1} + X_6\Psi_l^{n-1} + Y_6\Psi_l^{n-3} + Z_6\Psi_l^{n-5} + \left[(n-7) + \frac{(n-6)Z_5}{2n-11}\right]\Psi_l^{n-7} + \frac{n(n+1)(n+2)(n+3)(n+4)(n+5)(n+6)(n+7)}{(2n+1)(2n+3)(2n+5)(2n+7)(2n+9)(2n+11)(2n+13)}\Psi_l^{n+7}$$

$$U_1 = \left[(n-2) + \frac{(n-1)^2}{2n-1} + \frac{n^2(n-1)}{(2n-1)(2n+1)}\right]$$

$$V_1 = \left[\frac{n(n-1)}{2n-1} + \frac{n^3}{(2n-1)(2n+1)} + \frac{n(n+1)^2}{(2n+1)(2n+3)}\right]$$

$$U_2 = \left[\frac{n(n+1)(n+2)^2}{(2n+1)(2n+3)(2n+5)} + \frac{(n+1)V_1}{(2n+1)}\right]$$

$$V_2 = \left[\frac{(n-1)U_1}{(2n-3)} + \frac{nV_1}{(2n+1)}\right]$$

$$W_2 = \left[(n-3) + \frac{(n-2)U_1}{2n-3}\right]$$

$$U_3 = \left[\frac{n(n+1)(n+2)(n+3)^2}{(2n+1)(2n+3)(2n+5)(2n+7)} + \frac{(n+2)U_2}{(2n+3)}\right]$$

$$V_3 = \left[\frac{(n+1)U_2}{(2n+3)} + \frac{nV_2}{(2n-1)}\right]$$

$$W_3 = \left[\frac{(n-1)V_2}{(2n-1)} + \frac{(n-2)W_2}{(2n-5)}\right]$$

$$X_3 = \left[(n-4) + \frac{(n-3)W_2}{2n-5}\right]$$

$$U_4 = \left[\frac{n(n+1)(n+2)(n+3)(n+4)^2}{(2n+1)(2n+3)(2n+5)(2n+7)(2n+9)} + \frac{(n+3)U_3}{(2n+5)}\right]$$

$$V_4 = \left[\frac{(n+2)U_3}{(2n+5)} + \frac{(n+1)V_3}{(2n+1)}\right]$$

$$W_4 = \left[\frac{nV_3}{(2n+1)} + \frac{(n-1)W_3}{(2n-3)}\right]$$

$$X_4 = \left[\frac{(n-2)W_3}{(2n-3)} + \frac{(n-3)X_3}{(2n-7)}\right]$$

$$Y_4 = \left[(n-5) + \frac{(n-4)X_3}{2n-7}\right]$$

$$U_5 = \left[\frac{n(n+1)(n+2)(n+3)(n+4)(n+5)^2}{(2n+1)(2n+3)(2n+5)(2n+7)(2n+9)(2n+11)} + \frac{(n+4)U_4}{(2n+7)}\right]$$

$$V_5 = \left[\frac{(n+3)U_4}{(2n+7)} + \frac{(n+2)V_4}{(2n+3)}\right]$$

$$W_5 = \left[\frac{(n+1)V_4}{(2n+3)} + \frac{nW_4}{(2n-1)}\right]$$

$$X_5 = \left[\frac{(n-1)W_4}{(2n-1)} + \frac{(n-2)X_4}{(2n-5)}\right]$$

$$Y_5 = \left[\frac{(n-3)X_4}{(2n-5)} + \frac{(n-4)Y_4}{(2n-9)}\right]$$

$$Z_5 = \left[(n-6) + \frac{(n-5)Y_4}{2n-9}\right]$$

$$V_6 = \left[\frac{(n+4)U_5}{(2n+9)} + \frac{(n+3)V_5}{(2n+5)}\right]$$

$$U_6 = \left[\frac{n(n+1)(n+2)(n+3)(n+4)(n+5)(n+6)^2}{(2n+1)(2n+3)(2n+5)(2n+7)(2n+9)(2n+11)(2n+13)} + \frac{(n+5)U_5}{(2n+9)}\right]$$

$$W_6 = \left[\frac{(n+2)V_5}{(2n+5)} + \frac{(n+1)W_5}{(2n+1)}\right]$$

$$X_6 = \left[\frac{nW_5}{(2n+1)} + \frac{(n-1)X_5}{(2n-3)}\right]$$

$$Y_5 = \left[\frac{(n-2)X_5}{(2n-3)} + \frac{(n-3)Y_5}{(2n-7)}\right]$$

$$Z_6 = \left[\frac{(n-4)Y_5}{(2n-7)} + \frac{(n-5)Z_5}{2n-11}\right]$$

Finally, the expressions of $x^q \frac{\partial^2 P_n(\chi)}{\partial \chi^2}$ are derived in Eq. (A-4):

$$\begin{aligned}
\chi \frac{\partial^2 u}{\partial \chi^2} &= \sum_{n=0}^{N-1} \Psi_l^n \chi \frac{\partial^2 P_n(\chi)}{\partial \chi^2} = \sum_{n=0}^{N-3} R_l^n P_n(\chi) \\
\chi^2 \frac{\partial^2 u}{\partial \chi^2} &= \sum_{n=0}^{N-1} \Psi_l^n \chi^2 \frac{\partial^2 P_n(\chi)}{\partial \chi^2} = \sum_{n=0}^{N-3} S_l^n P_n(\chi) \\
\chi^3 \frac{\partial^2 u}{\partial \chi^2} &= \sum_{n=0}^{N-1} \Psi_l^n \chi^3 \frac{\partial^2 P_n(\chi)}{\partial \chi^2} = \sum_{n=0}^{N-3} T_l^n P_n(\chi) \\
\chi^4 \frac{\partial^2 u}{\partial \chi^2} &= \sum_{n=0}^{N-1} \Psi_l^n \chi^4 \frac{\partial^2 P_n(\chi)}{\partial \chi^2} = \sum_{n=0}^{N-3} U_l^n P_n(\chi) \\
\chi^5 \frac{\partial^2 u}{\partial \chi^2} &= \sum_{n=0}^{N-1} \Psi_l^n \chi^5 \frac{\partial^2 P_n(\chi)}{\partial \chi^2} = \sum_{n=0}^{N-3} V_l^n P_n(\chi) \\
\chi^6 \frac{\partial^2 u}{\partial \chi^2} &= \sum_{n=0}^{N-1} \Psi_l^n \chi^6 \frac{\partial^2 P_n(\chi)}{\partial \chi^2} = \sum_{n=0}^{N-3} W_l^n P_n(\chi) \\
\chi^7 \frac{\partial^2 u}{\partial \chi^2} &= \sum_{n=0}^{N-1} \Psi_l^n \chi^7 \frac{\partial^2 P_n(\chi)}{\partial \chi^2} = \sum_{n=0}^{N-3} X_l^n P_n(\chi) \\
\chi^8 \frac{\partial^2 u}{\partial \chi^2} &= \sum_{n=0}^{N-1} \Psi_l^n \chi^8 \frac{\partial^2 P_n(\chi)}{\partial \chi^2} = \sum_{n=0}^{N-3} Y_l^n P_n(\chi)
\end{aligned} \tag{A-4}$$

where

$$R_l^n = \left(\frac{2m+1}{2}\right) \sum_{n=m+1,m+3,\ldots}^{N-1} (n(n+1) - m(m+1) - 2)\Psi_l^n$$

$$S_l^m = m(m-1)\Psi_l^m + \left(\frac{2m+1}{2}\right) \sum_{n=m+2,m+4,\ldots}^{N-1} (n(n+1) - m(m+1) - 4)\Psi_l^n$$

$$T_l^n = \frac{n(n-1)(n+1)}{(2n+1)}\Psi_l^{n+1} + A_1\Psi_l^{n-1} + B_1\Psi_l^{n-3} + C_1\Psi_l^{n-5} + D_1\Psi_l^{n-7} + E_1\Psi_l^{n-9} + F_1\Psi_l^{n-11} + G_1\Psi_l^{n-13} + \ldots$$

$$U_l^n = \frac{n(n-1)(n+1)(n+2)}{(2n+1)(2n+3)}\Psi_l^{n+2} + A_2\Psi_l^n + B_2\Psi_l^{n-2} + C_2\Psi_l^{n-4} + D_2\Psi_l^{n-6} + E_2\Psi_l^{n-8} + F_2\Psi_l^{n-10} + G_2\Psi_l^{n-12} + \frac{(n-13)G_1}{2n-25}\Psi_l^{n-14} + \ldots$$

$$V_l^n = \frac{n(n-1)(n+1)(n+2)(n+3)}{(2n+1)(2n+3)(2n+5)}\Psi_l^{n+3} + A_3\Psi_l^{n+1} + B_3\Psi_l^{n-1} + C_3\Psi_l^{n-3} + D_3\Psi_l^{n-5} + E_3\Psi_l^{n-7} + F_3\Psi_l^{n-9} + G_3\Psi_l^{n-11} + H_3\Psi_l^{n-13} + \frac{(n-13)(n-14)G_1}{(2n-25)(2n-27)}\Psi_l^{n-15} + \ldots$$

$$W_l^n = \frac{n(n-1)(n+1)(n+2)(n+3)(n+4)}{(2n+1)(2n+3)(2n+5)(2n+7)}\Psi_l^{n+4} + A_4\Psi_l^{n+2} + B_4\Psi_l^n + C_4\Psi_l^{n-2} + D_4\Psi_l^{n-4} + E_4\Psi_l^{n-6} + F_4\Psi_l^{n-8} + G_4\Psi_l^{n-10} + H_4\Psi_l^{n-12} + I_4\Psi_l^{n-14} + \frac{(n-13)(n-14)(n-15)G_1}{(2n-25)(2n-27)(2n-29)}\Psi_l^{n-16} + \ldots$$

$$X_l^n = \frac{n(n-1)(n+1)(n+2)(n+3)(n+4)(n+5)}{(2n+1)(2n+3)(2n+5)(2n+7)(2n+9)}\Psi_l^{n+5} + A_5\Psi_l^{n+3} + B_5\Psi_l^{n+1} + C_5\Psi_l^{n-1} + D_5\Psi_l^{n-3} + E_5\Psi_l^{n-5} + F_5\Psi_l^{n-7} + G_5\Psi_l^{n-9} + H_5\Psi_l^{n-11} + I_5\Psi_l^{n-13} + J_5\Psi_l^{n-15} + \frac{(n-13)(n-14)(n-15)(n-16)G_1}{(2n-25)(2n-27)(2n-29)(2n-31)}\Psi_l^{n-17} + \ldots$$

$$Y_l^n = \frac{n(n-1)(n+1)(n+2)(n+3)(n+4)(n+5)(n+6)}{(2n+1)(2n+3)(2n+5)(2n+7)(2n+9)(2n+11)}\Psi_l^{n+6} + A_6\Psi_l^{n+4} + B_6\Psi_l^{n+2} + C_6\Psi_l^n + D_6\Psi_l^{n-2} + E_6\Psi_l^{n-4} + F_6\Psi_l^{n-6} + G_6\Psi_l^{n-8} + H_6\Psi_l^{n-10} + I_6\Psi_l^{n-12} + J_6\Psi_l^{n-14} + JJ\Psi_l^{n-16} + \frac{(n-13)(n-14)(n-15)(n-16)(n-17)G_1}{(2n-25)(2n-27)(2n-29)(2n-31)(2n-33)}\Psi_l^{n-18} + \ldots$$

$$H_3 = \left[\frac{(n-12)G_2}{2n-23} + \frac{(n-13)^2 G_1}{(2n-25)(2n-27)}\right]$$

$$A_4 = \left[\frac{n(n-1)(n+1)(n+2)(n+3)^2}{(2n+1)(2n+3)(2n+5)(2n+7)} + \frac{(n+2)A_3}{2n+3}\right]$$

$$B_4 = \left[\frac{(n+1)A_3}{2n+3} + \frac{nB_3}{2n-1}\right]$$

$$C_4 = \left[\frac{(n-1)B_3}{2n-1} + \frac{(n-2)C_3}{2n-5}\right]$$

$$D_4 = \left[\frac{(n-3)C_3}{2n-5} + \frac{(n-4)D_3}{2n-9}\right]$$

$$E_4 = \left[\frac{(n-5)D_3}{2n-9} + \frac{(n-6)E_3}{2n-13}\right]$$

$$F_4 = \left[\frac{(n-7)E_3}{2n-13} + \frac{(n-8)F_3}{2n-17}\right]$$

$$G_4 = \left[\frac{(n-9)F_3}{2n-17} + \frac{(n-10)G_3}{2n-21}\right]$$

$$H_4 = \left[\frac{(n-11)G_3}{2n-21} + \frac{(n-12)H_3}{2n-25}\right]$$

$$I_4 = \left[\frac{(n-13)H_3}{2n-25} + \frac{(n-13)(n-14)^2 G_1}{(2n-25)(2n-27)(2n-29)}\right]$$

$$A_5 = \left[\frac{n(n-1)(n+1)(n+2)(n+3)(n+4)^2}{(2n+1)(2n+3)(2n+5)(2n+7)(2n+9)} + \frac{(n+3)A_4}{2n+5}\right]$$

$$B_5 = \left[\frac{(n+2)A_4}{2n+5} + \frac{(n+1)B_4}{2n+1}\right]$$

$$C_5 = \left[\frac{nB_4}{2n+1} + \frac{(n-1)C_4}{2n-3}\right]$$

$$D_5 = \left[\frac{(n-2)C_4}{2n-3} + \frac{(n-3)D_4}{2n-7}\right]$$

$$E_5 = \left[\frac{(n-4)D_4}{2n-7} + \frac{(n-5)E_4}{2n-11}\right]$$

$$F_5 = \left[\frac{(n-6)E_4}{2n-11} + \frac{(n-7)F_4}{2n-15}\right]$$

$$G_5 = \left[\frac{(n-8)F_4}{2n-15} + \frac{(n-9)G_4}{2n-19}\right]$$

$$H_5 = \left[\frac{(n-10)G_4}{2n-19} + \frac{(n-11)H_4}{2n-23}\right]$$

$$I_5 = \left[\frac{(n-12)H_4}{2n-23} + \frac{(n-13)I_4}{2n-27}\right]$$

$$J_5 = \left[\frac{(n-14)I_4}{2n-27} + \frac{(n-13)(n-14)(n-15)^2 G_1}{(2n-25)(2n-27)(2n-29)(2n-31)}\right]$$

$$A_6 = \left[\frac{n(n-1)(n+1)(n+2)(n+3)(n+4)(n+5)^2}{(2n+1)(2n+3)(2n+5)(2n+7)(2n+9)(2n+11)} + \frac{(n+4)A_5}{2n+7}\right]$$

$$B_6 = \left[\frac{(n+3)A_5}{2n+7} + \frac{(n+2)B_5}{2n+3}\right]$$

$$C_6 = \left[\frac{(n+1)B_5}{2n+3} + \frac{nC_5}{2n-1}\right]$$

$$D_6 = \left[\frac{(n-1)C_5}{2n-1} + \frac{(n-2)D_5}{2n-5}\right]$$

$$E_6 = \left[\frac{(n-3)D_5}{2n-5} + \frac{(n-4)E_5}{2n-9}\right]$$

$$F_6 = \left[\frac{(n-5)E_5}{2n-9} + \frac{(n-6)F_5}{2n-13}\right]$$

$$G_6 = \left[\frac{(n-7)F_5}{2n-13} + \frac{(n-8)G_5}{2n-17}\right]$$

$$H_6 = \left[\frac{(n-9)G_5}{2n-17} + \frac{(n-10)H_5}{2n-21}\right]$$

$$I_6 = \left[\frac{(n-11)H_5}{2n-21} + \frac{(n-12)I_5}{2n-25}\right]$$

References

[1] Ankit Gupta, M. Talha, Recent development in modeling and analysis of functionally graded materials and structures [J], Prog. Aerosp. Sci. 79 (2015) 1–14.
[2] C.F. He, M.F. Zheng, y. Lv, Development, applications and challenges in ultrasonic guided waves testing technology [J], Chinese J. Sci. Instrum. 37 (8) (2016) 1713–1735.
[3] J. Guo, J. Chen, E. Pan, Size-dependent behavior of functionally graded anisotropic composite plates [J], Int. J. Eng. Sci. 106 (2016) 110–124.
[4] J. Guo, J. Chen, E. Pan, A three-dimensional size-dependent layered model for simply-supported and functionally graded magnetoelectroelastic plates [J], Acta Mech. Solida Sin. 31 (5) (2018) 652–671.
[5] J. Sladek, V. Sladek, S. Krahulec, Enhancement of the magnetoelectric coefficient in functionally graded multiferroic composites [J], J. Intell. Mater. Syst. Struct. 23 (14) (2012) 1649–1658.
[6] J. Sladek, V. Sladek, S. Krahulec, Analyses of functionally graded plates with a magnetoelectroelastic layer [J], Smart Mater. Struct. 22 (3) (2013) 035003.
[7] R. Wang, E. Pan, Three-dimensional modeling of functionally graded multiferroic composites [J], Mech. Adv. Mater. Struct. 18 (1) (2011) 68–76.
[8] P.L. Bishay, B. Sampat, J. Sladek, Effect of lattice mismatch strain grading on the electromechanical behavior of functionally graded quantum dots [C], Key Eng. Mater. 759 (2018) 71–75.
[9] G.R. Liu, J. Tani, T. Ohyoshi, Lamb waves in a functionally gradient material plate and its transient response, Part 1: Theory, Part 2: Calculation results, Trans. Jpn Soc. Mech. Eng. 57 (A) (1991) 603–611.
[10] T. Ohyoshi, Linearly inhomogeneous layer element for reflectance evaluation of inhomogeneous layers, Dyn. Response Behav. Compos. 46 (2) (1995) 121–126.
[11] G.R. Liu, X. Han, K.Y. Lam, Stress waves in functionally gradient materials and its use for material characterization [J], Composites Part B 30 (4) (1999) 383–394.
[12] X. Han, G.R. Liu, K.Y. Lam, A quadratic layer element for analyzing stress waves in FGMs and its application in material characterization [J], J. Sound Vib. 236 (2) (2000) 307–321.
[13] W.Q. Chen, H.J. Ding, Bending of functionally graded piezoelectric rectangular plates [J], Acta Mech. Solida Sin. 4 (2000) 312–319.
[14] W.Q. Chen, H.M. Wang, R.H. Bao, On calculating dispersion curves of waves in a functionally graded elastic plate [J], Compos. Struct. 81 (2) (2007) 233–242.
[15] Issam B Salah, Y. Wali, M.H. Ben Ghozlen, Love waves in functionally graded piezoelectric materials by stiffness matrix method [J], Ultrasonics 51 (3) (2011) 310–316.
[16] X.Y. Li, Z.K. Wang, S.H. Huang, Love waves in functionally graded piezoelectric materials [J], Int. J. Solids Struct. 41 (2004) 7309–7328.
[17] Z.H. Qian, F. Jin, Z.K. Wang, K. Kishimoto, Transverse surface waves on a piezoelectric material carrying a functionally graded layer of finite thickness [J], Int. J. Eng. Sci. 45 (2007) 455–466.
[18] J.E. Lefebvre, V. Zhang, Joseph Gazalet, et al., Acoustic wave propagation in continuous functionally graded plates: an extension of the Legendre polynomial approach, IEEE Trans. Ultrason. Ferroelectr. Freq. Control 48 (5) (2001) 1332–1340.
[19] L. Elmaimouni, J.E. Lefebvre, V. Zhang, et al., Guided waves in radially graded cylinders: a polynomial approach [J], NDT&E International 38 (3) (2005) 344–353.
[20] J. Yu, B. Wu, C. He, Guided thermoelastic waves in functionally graded plates with two relaxation times [J], Int. J. Eng. Sci. 48 (12) (2010) 1709–1720.
[21] J.G. Yu, F.E. Ratolojanahary, J.E. Lefebvre, Guided waves in functionally graded viscoelastic plates [J], Compos. Struct. 93 (11) (2011) 2671–2677.
[22] X.M. Zhang, Z. Li, J.G. Yu, The computation of complex dispersion and properties of evanescent lamb wave in functionally graded piezoelectric-piezomagnetic plates [J], Materials 11 (7) (2018) 1186.
[23] X.S. Cao, F. Jin, I. Jeon, Calculation of propagation properties of Lamb waves in a functionally graded material (FGM) plate by power series technique [J], NDT&E Int. 44 (1) (2011) 84–92.
[24] X.S. Cao, F. Jin, Z.K. Wang, On dispersion relations of Rayleigh waves in a functionally graded piezoelectric material (FGPM) half-space [J], Acta Mech. 200 (2008) 247–261.
[25] S. Hedayatrasa, T.Q. Bui, C.Z. Zhang, Numerical modeling of wave propagation in functionally graded materials using time-domain spectral Chebyshev elements [J], J. Comput. Phys. 258 (2014) 381–404.
[26] F. Hernando Quintanilla, Z. Fan, M.J.S. Lowe, R.V. Craster, Guided waves' dispersion curves in anisotropic viscoelastic single-and multi-layered media [J], Proc. Roy. Soc. A: Math. Phys. Eng. Sci. 471 (2183) (2015) 20150268.
[27] M.V. Predoi, M. Castaings, B. Hosten, C. Bacon, Wave propagation along transversely periodic structures [J], J. Acoust. Soc. Am. 121 (4) (2007) 1935–1944.
[28] P. Zuo, X. Yu, Z. Fan, Numerical modeling of embedded solid waveguides using SAFE-PML approach using a commercially available finite element package [J], NDT E Int. 90 (2017) 11–23.
[29] M.F. Zheng, C.F. He, Y. Lu, et al., State-vector formalism and the Legendre polynomial solution for modelling guided waves in anisotropic plates [J], J. Sound Vib. 412 (2018) 372–388.
[30] M.F. Zheng, C.F. He, Y. Lu, et al., Guided waves propagation in anisotropic hollow cylinders by Legendre polynomial solution based on state-vector formalism [J], Compos. Struct. 207 (2019) 645–657.
[31] X. Han, G.R. Liu, Elastic waves in a functionally graded piezoelectric cylinder [J], Smart Mater. Struct 12 (2003) 962–971.
[32] Ke Hong, Analysis of Lamb waves propagation in functional gradient materials using Taylor expansion method [J], Acta Physica Sinica 60 (10) (2011) 104303.